Supporting Information

Sulfonated Perylene-Based Conjugated Microporous Polymer as High-Performance Adsorbent to Photo-Enhanced Uranium Extraction from Seawater

Fengtao Yu,* Fangru Song, Runze Wang, Mei Xu and Feng Luo*

State Key Laboratory of Nuclear Resources and Environment, School of Chemistry, Biology and Materials Science, East China University of Technology, Nanchang, 330013, P. R. China.

* Corresponding author

E-mail addresses: fty853815622@ecut.edu.cn

E-mail addresses: ecitluofeng@163.com

Table of contents

1. Supporting Experimental Section

1.1 Chemicals

The perylene-based monomer of 2,5,8,11-tetrakis(4,4,5,5-tertramethyl-1,3,2-dioxaborolan-2-yl)perylene is synthesized by a modified method according to previous paper.[S1] 1,4-dibromobenzene, tetrakis(triphenylphosphine)palladium(0) ($Pd(PPh_3)_4$), potassium carbonate (K_2CO_3), chlorosulfonic acid and anhydrous N,N-dimethylformamide (DMF) were purchased from Energy Chemical. All the purchased reagents are of analytical grade and used without further purification, unless otherwise noted.

1.2 Materials synthesis

1.2.1 The synthesis of 2,5,8,11-tetrakis(4,4,5,5-tetramethyl-1,3,2-dioxaborolan-2-yl)perylene. Under N_2 atmosphere, perylene (499 mg, 1.98 mmol), 4,4,4',4',5,5,5',5'-octamethyl-2,2'-bi(1,3,2-dioxaborolane) (2215 mg, 8.7 mmol), $[Ir(OMe)COD]_2$ (65.6 mg, 0.1 mmol) and 4,4'-dimethyl-2,2'-bipyridyl (54.4 mg, 0.2 mmol) are dissolved in 20 mL ultra-dry THF solution. Subsequently, the mixture is heated at 80 ℃ for 17 h. After cooling to room temperature (RT), the reaction mixture is dropped into 100 mL of methanol, obvious solid precipitation is observed. The product is collected by vacuum filtration and washed multiple times with methanol to give a light-yellow solid (3200 mg, 88%). ^{1}HNMR (400 MHz, $CDCl_3$, ppm) δ: 8.63 (s, 4H), 8.25 (s, 4H), 1.43 (s, 48H) ^{13}CNMR (100 MHz, $CDCl_3$, ppm) δ:136.94, 133.29, 131.96, 130.38, 126.05, 84.03, 24.96. MS (ESI-MS) m/z calcd. For $C_{44}H_{56}B_4O_8$: 795.39. [M + K]. Found: 795.40.

1.2.2 The synthesis of PyB. The CMP of PyB was synthesized by Pd(0)–catalyzed Suzuki–Miyaura cross coupling polycondensation reaction. In brief, 1,3,6,8-tetrabromopyrene (756.4 mg, 1.0 mmol), 1,4-dibromobenzene (471.8 mg, 2.0 mmol), $Pd(PPh_3)_4$ (23 mg, 0.02 mmol), K_2CO_3 aqueous solution (2 M, 3 mL) and DMF (30 mL) are added into a dry round-bottomed flask (100 mL). The reaction mixture is degassed by freeze-pump-thaw technique for three times and sealed under vacuum, and then heated to 150 ºC for 48 h, and then cooled down to room temperature (RT). The resulting reaction solution is poured into deionized water and collected by filtration.

The solids are washed with CH_3OH, H_2O and acetone and then purified using a Soxhlet apparatus with chloroform and THF sequentially until the extracts appeared colorless to afford the targeted CMPs (marked as PyB, a dark-yellow solid) after complete drying in vacuum.

1.2.3 The synthesis of PyB-SO_3H. The sulfonated conjugated microporous polymer is obtained by a classic aromatic sulfonation organic reaction with PyB and chloro-sulfonic acid. In short, PyB (300 mg) is placed in a round bottom flask (100 mL) with dichloromethane (30 mL), the mixture is maintained at 273.15 K with an ice bath. Subsequently, chloro-sulfonic acid (3.0 mL) is added dropwise within 30 min. Then, the reaction system gradually warms to RT and stirred for 72 h. After the reaction, the resulting solution is poured into ice, and the precipitation is filtered and washed with water and CH_3OH. The sulfonate-grafted product (marked as PyB-SO_3H, an orange red solid) is obtained after complete drying in vacuum.

1.2.4 Materials characterization. ^1H NMR (400 MHz) and ^{13}C NMR (100 MHz) spectra are obtained in deuterated solvents on Bruker AM-400 MHz with tetramethylsilane (TMS) as an internal standard. High-resolution mass spectrometry (HRMS) testing is carried out using a Waters LCT Premier XE spectrometer. Thermogravimetric analysis (TGA) is performed using a TGA Q600 thermal analysis system under air atmosphere with a heating rate of 10 °C/min. ^{13}C CP/MAS solid-state NMR spectra of are acquired from a Bruker Avance III 400 spectrometer. The Powder X-ray diffraction (PXRD) patterns of the CMPs were collected on a Bruker D8 Advance X-ray powder diffractometer (Cu Kα X-ray source) operating at a voltage of 40 kV and a current of 30 mA. Field-emission scanning electron microscope (FE-SEM) images are taken by Nova Nanosem 450. Energy-dispersive X-ray spectroscopy (EDS) are conducted using SEM equipped with an EDS detector. X-ray Photoelectron Spectroscopy (XPS) data are obtained on a Perkin-Elmer PHI 5000C ESCA system with Al Kα radiation operated at 250 W. All binding energies are referenced to the C 1s peak at 284.6 eV. The Fourier-transform infrared (FT-IR) spectra are recorded on a Nicolet Impact 410 FT-IR spectrometer. UV-vis diffuse reflection spectrum (DRS) are obtained by UV-vis spectrophotometer (UV-2550, Shimadzu, Japan). The nitrogen

adsorption/desorption isotherms are measured at 77 K and ammonia adsorption/desorption isotherms are measured at 298 K using a Micromeritics ASAP 2020 gas adsorption analyzers. The samples are outgassed at 100 °C for 12 h before the measurements. Surface areas are calculated from the adsorption data using Brunauer-Emmett-Teller4 (BET) methods. The pore-size-distribution curves are obtained via the non-local density functional theory (NLDFT) method. Electron spin resonance (ESR) spectra are recorded on a Bruker A300 spectrometer. The 5,5-dimethyl-1-pyrroline-N-oxide (DMPO) is used to trap the superoxide radical ($\cdot O_2^-$) and the 2,2,6,6-tetramethylpiperidine (TEMP) is used to detect singlet oxygen ($^1O_2$). The stead-state photoluminescence (PL) spectra of samples are measured on a Perkin-Elmer LS 55 at room temperature. Time-correlated single photon counting is performed on Edinburgh Instruments FLS 920 fluorescence spectrometer.

1.2.5 Electrochemical measurements. Transient photocurrent responses (I–t) and electrochemical impedance spectra (EIS) of the obtained samples are investigated on a CHI650E electrochemical workstation with in a conventional three-electrode-cell system. An aqueous solution of 0.5 M Na_2SO_4 is used as the supporting electrolyte and a 300 W Xe-lamp with a cutoff filter ($\lambda \geq 400$ nm) served as the light source. The films electrodes are prepared as follows: 25 mg of the as-synthesized samples (PyB and PyB-SO_3H) is separately ground with 10 μL of a Nafion (5%) aqueous solution and 50 μL of ethanol to make slurry. The slurry is then coated onto ITO glass electrodes with an active area of 0.25 cm^2, and these electrolytes are dried at 120 °C for 1 h to evaporate the solvent in muffle furnace. The photocurrent intensity of as-prepared electrodes is measured at 0 V versus Ag/AgCl with the light on and off. EIS is determined over the frequency range of 10^2–10^6 Hz with an ac amplitude of 10 mV at the open circuit voltage under room-light illumination.

1.2.6 Adsorption and Photocatalysis in removing U(VI). All uranium removal experiments are conducted in a jacketed quartz beaker photoreactor cooled by circulating water (Instrument Model: CEL-APR250H). For high concentration solutions, the concentration is tested by the Arsenazo III method. For low concentration solutions, the concentration is detected by inductively coupled plasma emission

spectrometer (ICP-OES). A stock solution of uranyl nitrate (500 ppm) is prepared by dissolving appropriate amounts of $UO_2(NO_3)_2 \cdot 6H_2O$ in a suitable amount of deionized water. The pH value of the solutions was adjusted to 4.0 with HNO_3 or NaOH aqueous solution.

First, the adsorption performance in the dark of the obtained samples are evaluated. In general procedure, to obtain the uranium adsorption isotherms, 20 mg PyB or PyB-SO_3H is added into 100 mL solution of UO_2^{2+} with different concentrations. The mixture is sonication for 30 seconds and shaken for 120 min at ambient temperature to achieve sorption equilibrium. The adsorbed amount at equilibrium (q_e, mg g^{-1}) is calculated by the following equation:

$$q_e = \frac{(c_0 - c_e) \times V}{m} \quad \textbf{(1)}$$

where V is the volume of the treated solution (L), m is the amount of used adsorbent (g), and c_0 and c_e are the initial concentration and the final equilibrium concentration of uranium, respectively.

The equation of the Langmiur isotherm model is represented as following:

$$\frac{c_e}{q_e} = \frac{1}{q_m k_{L1}} + \frac{c_e}{q_m} \quad \textbf{(2)}$$

where q_m is the maximum adsorption when the adsorption reaches equilibrium, and k_L is a constant characterized by the affinity of the adsorbate with the adsorbent. The value of c_e/q_e as the function of c_e were plotted and fitted with a linear equation from which the q_m and k_L could be calculated according to the slope and intercept.

The Freundlich model is appropriate for multilayer sorption, which can be described as:

$$\ln q_e = \ln k_F + \frac{1}{n} \ln c_e \quad \textbf{(3)}$$

where k_F ($mg^{1-n}\ L^n/g$) denotes the Freundlich sorption coefficient, and n expresses how favorable the sorption process is. k_F and n are empirical coefficients.

In the kinetics studies: 20 mg PyB or PyB-SO_3H was added into 100 mL solution containing 50 ppm uranium and used 0.1 M HNO_3 to adjust the pH of the solution to 4.0. The mixture is stirred for a series of contact times, and the filtrate is collected at

different contact time. The adsorption capacity of uranium as a function of contact time is obtained to determine the kinetics curve. Pseudo-first-order kinetic model was described as the following function:

$$\ln(q_e - q_t) = \ln q_e - k_1 t \qquad \textbf{(4)}$$

where q_e (mg g^{-1}) represents the amount of U on the adsorbent under equilibrium, and k_1 (min^{-1}) is pseudo-first-order adsorption rate constant.

Pseudo-second-order kinetic model is described as the following function:

$$\frac{t}{q_t} = \frac{1}{k_s + q_e^2} + \frac{t}{q_e} \qquad \textbf{(5)}$$

where q_e (mg g^{-1}) represents the amount of U on the adsorbent under equilibrium, and k_s (g mg^{-1} min^{-1}) is pseudo-second-order adsorption rate constant.

In the photocatalytic removal of uranium studies: Typically, 20 mg photocatalyst is placed into 100 mL of aqueous solutions containing 50 ppm U(VI) at pH 4.0 and under stirring continuously. Before irradiation, the reaction system is continuously stirred to reach the adsorption-desorption equilibrium. Then, the suspension is illuminated using a 300 W Xe lamp (Light source model: SHX-F300, $\lambda \geq 400$ nm). Calculate the efficiency of photocatalytic reduction of uranium removal according to the following equation:

$$\mathrm{RE} = \frac{(C_0 - C_t)}{C_0} \times 100\% \qquad \textbf{(6)}$$

Where, RE is the uranium reduction efficiency; C_0 and C_t are the concentration (ppm, mg/L) of uranium at initial and contact time t (min), respectively.

In the experiments of recycling: after photoreduction reaction, photocatalyst is collected by centrifugation, and washes by the 1 M HNO_3 to eliminate UO_2 on the surface, and further washes with the deionized H_2O. Then, photocatalyst was dehydrated in vacuum at 60 ℃ for 8 h.

1.2.7 Practical application. For examining the realistic application, an inventory solution of 500 ppm U(VI) is spiked into the real seawater. Other processes are the same as above. The amounts of extracted uranium are calculated using the equation as follow:

$$q_t = \frac{(C_0 - C_t)V}{m} \qquad (7)$$

Where q_t is the amounts of extracted uranium (mg U/g CMPs); V is the volume of the solution (L), and m is the mass of the samples (g).

For the recycling experiment, the photocatalyst after the reaction is obtained through centrifugation, and washed with 1 M HNO_3 to eliminate UO_2 on the surface, and then washes with the deionized water. Then, the photocatalyst is dehydrated under vacuum at 60 ℃ for 8 h.

2. Supporting Figures

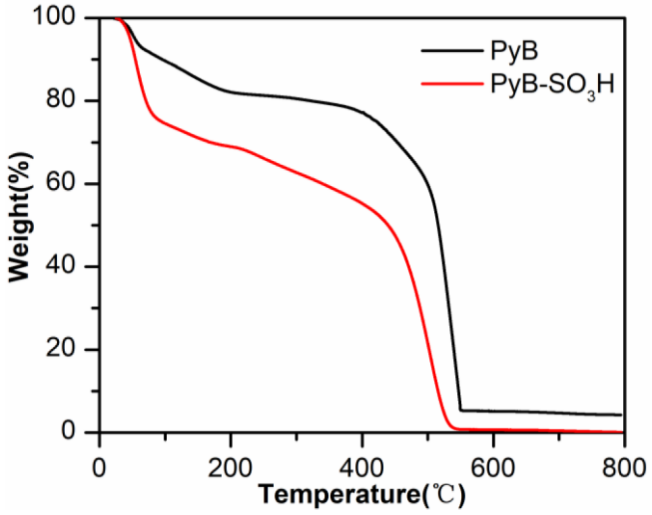

Fig.S1. Thermal gravimetric analysis of PyB and PyB-SO_3H in air atmosphere with a heating rate of 10 °C/min.

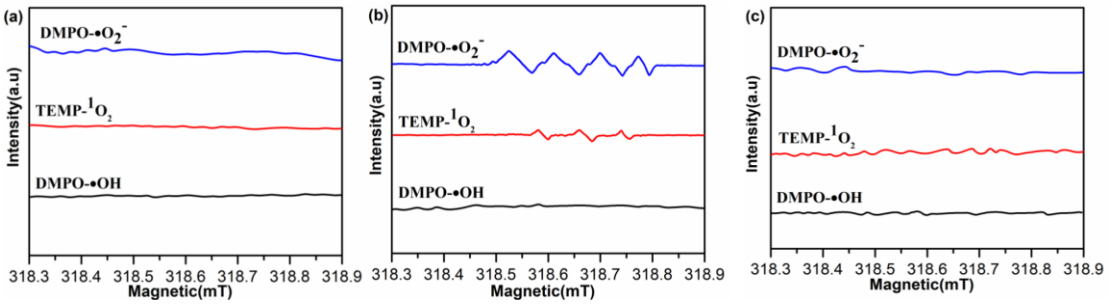

Fig.S2. (a) ESR spectra of the DMPO-•OH adducts, adduct of TEMP-$^1O_2$ and DMPO-•O_2^- adducts of PyB, recorded under dark; (b) ESR spectra of the DMPO-•OH adducts, adduct of TEMP-$^1O_2$ and DMPO-•O_2^- adducts of PyB, recorded under visible irradiation ($\lambda \geq 400$ nm); (c) ESR spectra of the DMPO-•OH adducts, adduct of TEMP-$^1O_2$ and DMPO-•O_2^- adducts of PyB-SO_3H, recorded under dark.

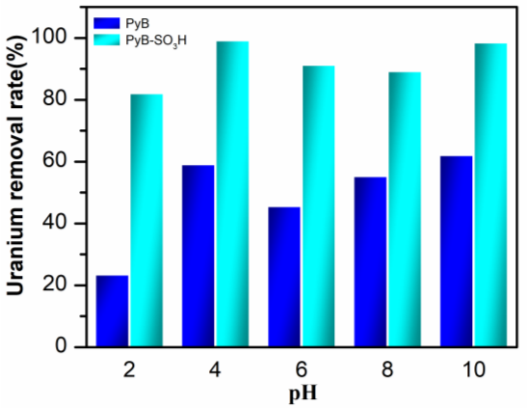

Fig.S3. Uranium removal rate of PyB and PyB-SO_3H at different pH.

Fig.S3 shows the uranium removal rate of PyB and PyB-SO_3H is significantly affected by the pH. Under acidic conditions, it affects the coordination of adsorbent and uranyl ions, and under alkaline conditions, it affects the existence of uranyl ions. Therefore, subsequent adsorption experiments are mostly carried out at pH 4.0.

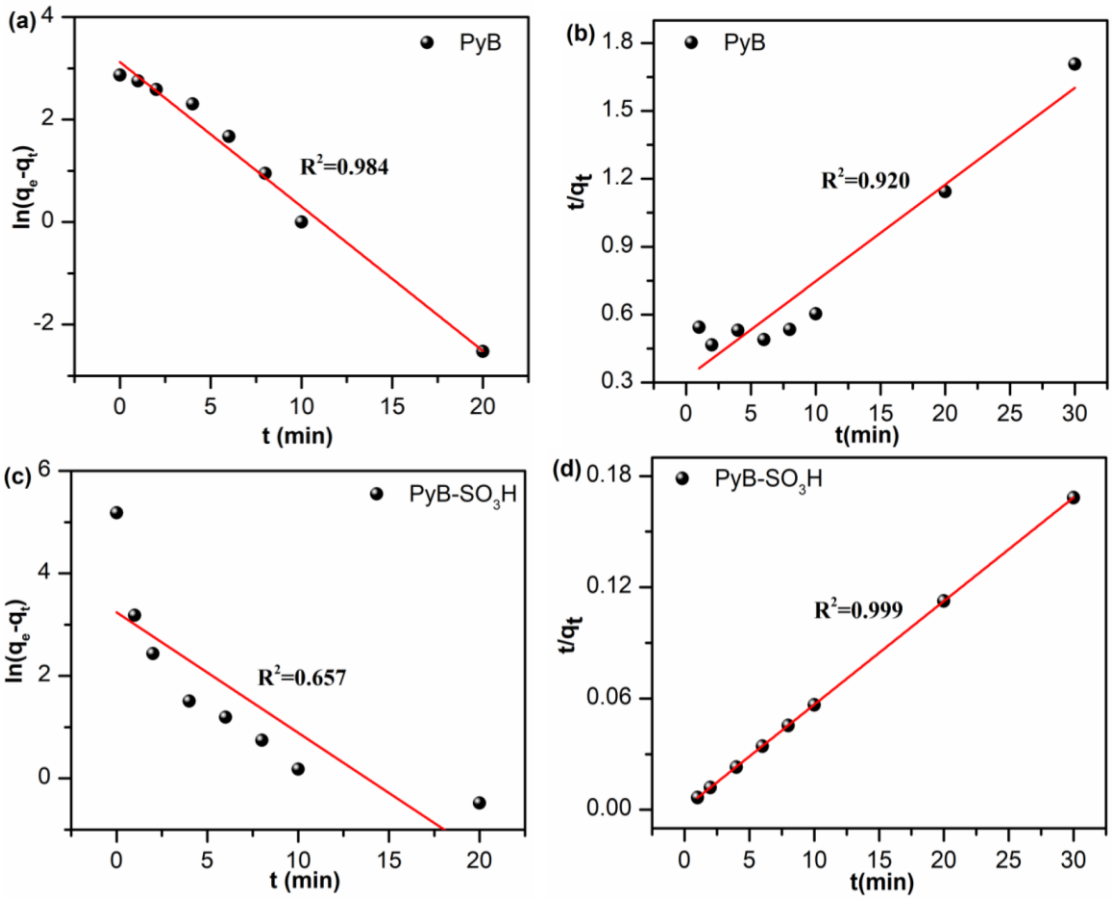

Fig.S4. (a) Pseudo-first-order; (b) Pseudo-second-order and model kinetic plots of adsorption uranium onto PyB; (c) Pseudo-first-order; (d) Pseudo-second-order and model kinetic plots of adsorption uranium onto PyB-SO_3H.

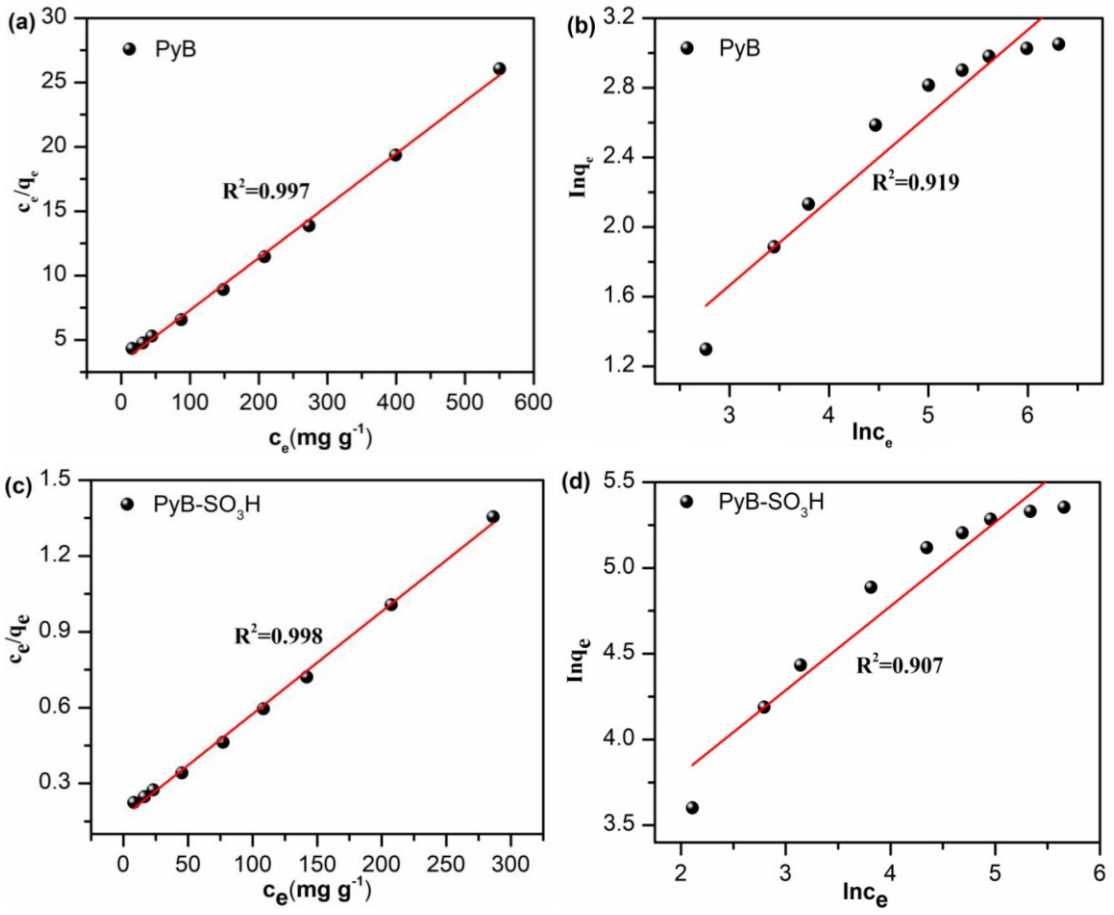

Fig.S5. (a) Langmuir model for the adsorption of uranium for PyB; (b) Freundlich model for the adsorption of uranium for PyB; (c) Langmuir model for the adsorption of uranium for PyB-SO_3H; (d) Freundlich model for the adsorption of uranium for PyB-SO_3H.

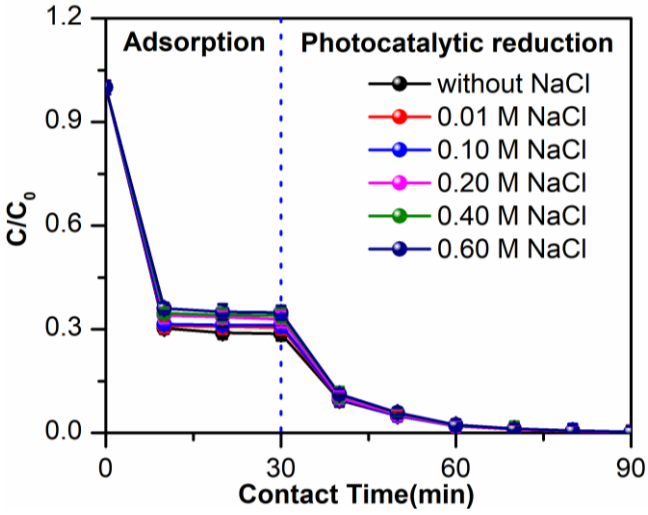

Fig.S6. The effect of NaCl concentration on U(VI) removal. Conditions: 100 mL water containing 10 mL methanol, 50 ppm U(VI) at pH 4.0, 20 mg of PyB-SO_3H under visible light.

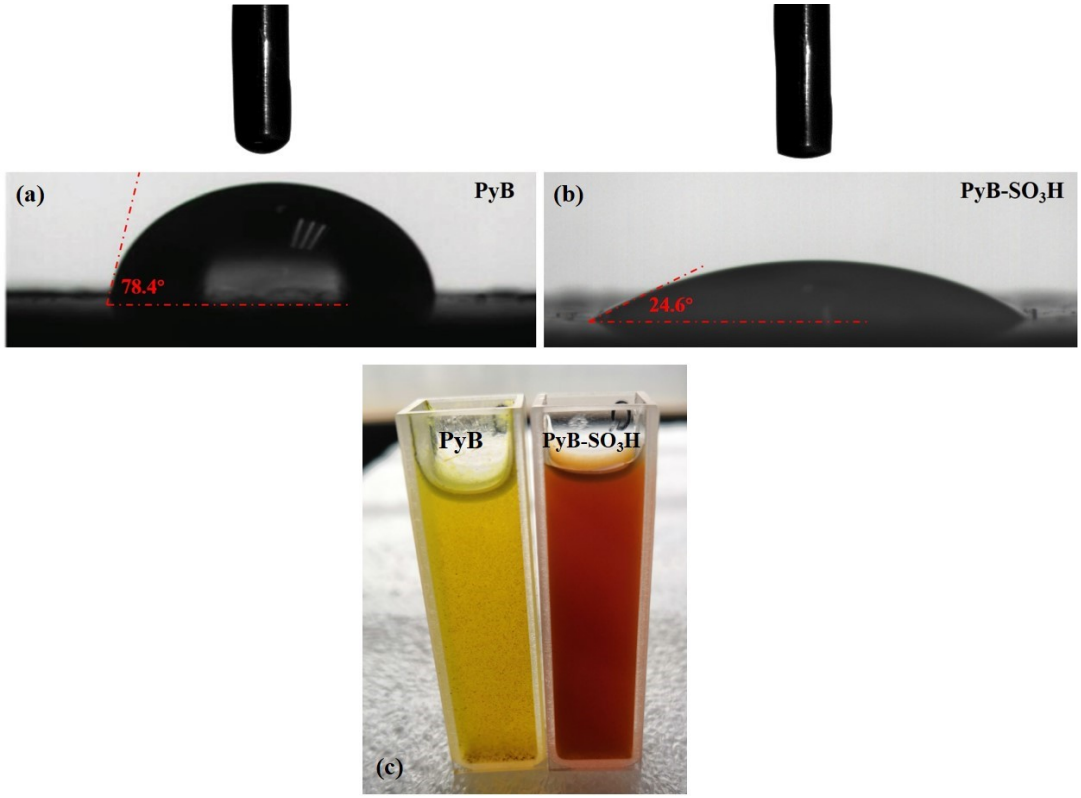

Fig.S7. (a and b) The water contact angle of PyB and PyB-SO_3H; (c) The dispersion of the PyB and PyB-SO_3H in aqueous solutions.

The water contact angle measurement is carried out to characterize the difference in hydrophilicity of PyB and PyB-SO_3H. As shown in Fig.S7, the contact angle of PyB-SO_3H is significantly reduced to 24.6°compared with PyB (78.4°), indicating that the introduction of sulfonic acid can significantly increase its hydrophilicity. This can promote the dispersion of the PyB-SO_3H in aqueous solutions while benefiting their contact with the hydrophilic targets in the adsorption applications. In addition, according to previously reported literature, the increase in hydrophilicity is conducive to the improvement of photocatalytic activity. [S2-S6]

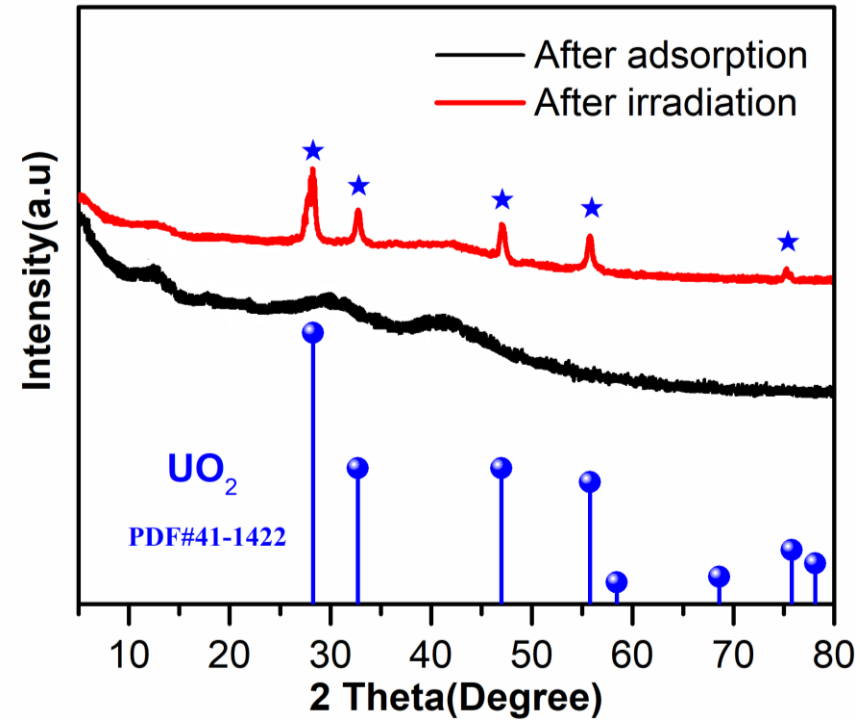

Fig.S8. XRD patterns of PyB-SO_3H before and after photoreduction with 50 ppm U(VI) at PH=4.

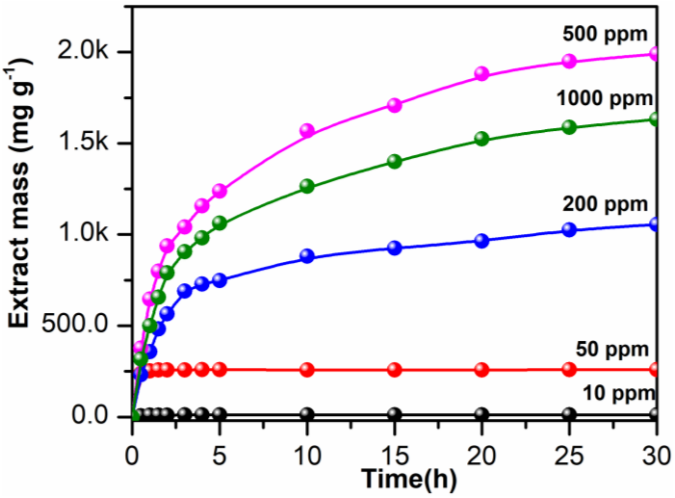

Fig.S9. Uranium extraction from spiked seawater with initial uranium concentrations of 10, 50, 200, 500 and 1000 ppm. (Reaction conditions: 100 mL real sea water containing 10 mL methanol, 20 mg of PyB-SO_3H under visible-light).

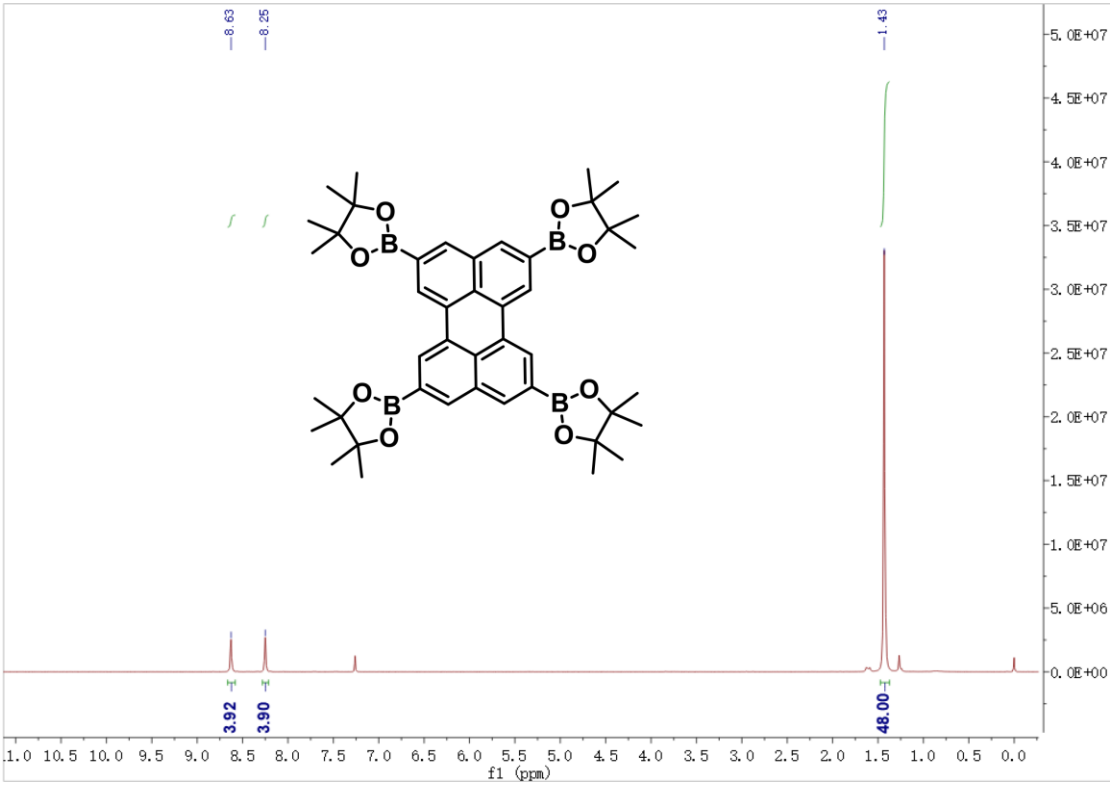

Fig.S10. The ^{1}HNMR spectrum of 2,5,8,11-tetrakis(4,4,5,5-tertramethyl-1,3,2-dioxaborolan-2-yl)perylene in deuterated chloroform.

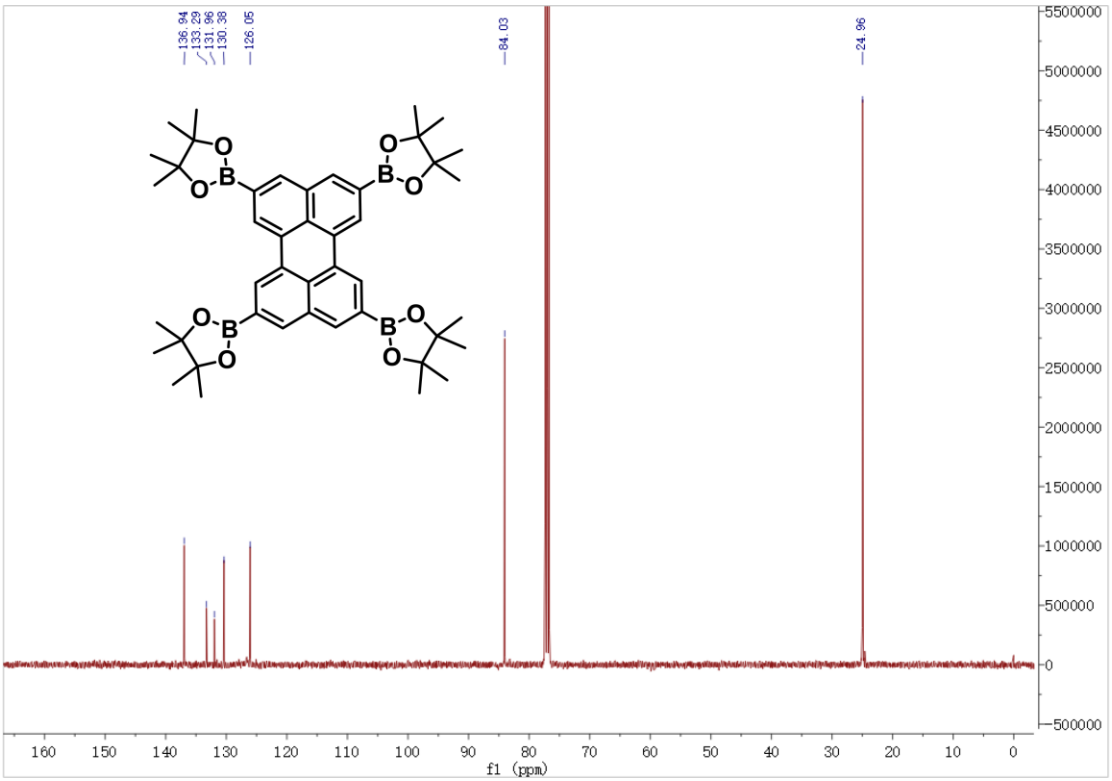

Fig.S11. The ^{13}CNMR spectrum of 2,5,8,11-tetrakis(4,4,5,5-tertramethyl-1,3,2-dioxaborolan-2-

yl)perylene in deuterated chloroform.

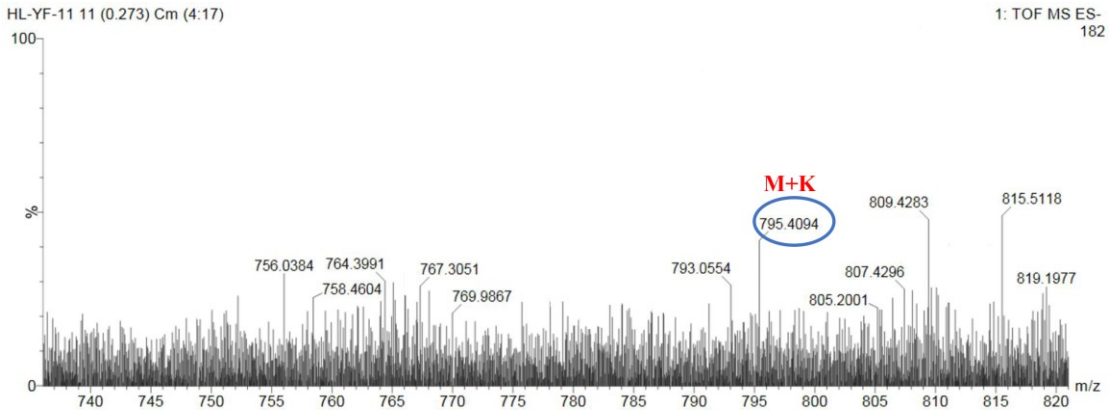

Fig.S12. High-resolution mass spectrometry of 2,5,8,11-tetrakis(4,4,5,5-tertramethyl-1,3,2-dioxaborolan-2-yl)perylene.

3. Supporting Tables

Table S1. Elemental composition (atom ratios) of samples according to XPS analysis.

Sample	C/at %	O/at %	S/at %	O/C
PyB	96.6	3.4	0	0.035
PyB-SO_3H	83.0	13.6	3.4	0.16

Table S2. Relative ratios of two carbon species determined by C 1s spectra for samples.

	C=C			C−S		
Sample	Binding Energy(eV)	area	%	Binding Energy(eV)	area	%
PyB	284.6	71783.64	100	/	/	/
PyB-SO_3H	284.6	32238.58	61.4	285.15	20262.45	38.6

Table S3. Relative ratios of four sulfur species determined by S2p spectra for the PyB-SO_3H.

Sample	S=O (-SO_3H)						Sulfide and Sulfite groups					
	$S2p_{1/2}$			$S2p_{3/2}$			$S2p_{1/2}$			$S2p_{3/2}$		
	Binding Energy (eV)	area	%	Binding Energy (eV)	area	%	Binding Energy (eV)	area	%	Binding Energy (eV)	area	%
PyB-SO_3H	169.0	3318.1	60.6	168.0	1659.0	30.3	164.6	334.7	6.1	163.7	167.4	3.0

Table S4. Relative ratios of two oxygen species determined by O1s spectra for samples.

	O−H			O=S		
Sample	Binding Energy(eV)	area	%	Binding Energy(eV)	area	%

PyB-SO_3H	532.95	10051.1	32.0	531.77	21376.2	68.0

Table S5. Kinetic parameters of pseudo-first-order and pseudo-second-order models of U adsorption by means of PyB and PyB-SO_3H.

Adsorbent	$q_{e,exp}$ (mg·g^{-1})	Pseudo-first-order			Pseudo-second-order		
		$q_{e,cal}$ (mg·g^{-1})	k_1 (min^{-1})	R^2	$q_{e,cal}$ (mg·g^{-1})	k_2 (g·mg^{-1}·min^{-1})	R^2
PyB	17.58	18.56	0.282	0.984	23.38	0.075	0.919
PyB-SO_3H	178.22	25.57	0.235	0.657	178.89	0.2	0.999

Table S6. Isotherm parameters of Langmuir and Freundlich models of U adsorption by means of PyB and PyB-SO_3H.

Adsorbent	$q_{e,exp}$ (mg·g^{-1})	Langmuir isotherm			Freundlich isotherm		
		$q_{e,cal}$ (mg·g^{-1})	K_L (L mg^{-1})	R^2	*1/n*	K_F (g^{-1}·mg$^{1-1/n}$·L$^{-1/n}$)	R^2
PyB	21.13	24.64	0.012	0.997	0.489	1.216	0.919
PyB-SO_3H	211.26	215.22	0.027	0.998	0.493	16.75	0.902

Table S7. Relative ratios of three oxygen species determined by O1s spectra for PyB-SO_3H after extracting of uranium.

Sample	O—H			O=S			O=U		
	Binding Energy(eV)	area	%	Binding Energy(eV)	area	%	Binding Energy(eV)	area	%
PyB-SO_3H	532.9	7868	23.3	531.8	23928.5	71	530.5	1901	5.6

Table S8. Relative ratios of two uranium species determined by U4f spectra for PyB-SO_3H after extracting of uranium under dark.

Sample	U(VI)					
	$U4f_{5/2}$			$U4f_{7/2}$		
	Binding Energy(eV)	area	%	Binding Energy(eV)	area	%
PyB-SO_3H	392.9	12550	40.6	382.3	18345	59.4

Table S9. Relative ratios of four uranium species determined by U4f spectra for PyB-SO_3H after extracting of uranium under visible-light irradiation.

Sample	U(VI)						U(IV)					
	$U4f_{5/2}$			$U4f_{7/2}$			$U4f_{5/2}$			$U4f_{7/2}$		
	Binding Energy (eV)	area	%	Binding Energy (eV)	area	%	Binding Energy (eV)	area	%	Binding Energy (eV)	area	%
PyB-SO_3H	392.9	4500	14	382.3	6543.5	20	392.3	9000	27	381.5	13087	39

References

[S1] Y. F. Xu, N. Mao, S. Feng, C. Zhang, F. Wang, Y. Chen, J. H. Zeng and J. X. Jiang, *Macromol. Chem. Phys.* 2017, **218**, 1700049–1700057.

[S2] H. N. Ye, Z. Q. Wang, Z. C. Yang, S. C. Zhang, X. Q. Gong and J. L. Hua, *J. Mater. Chem. A,* 2020, **8**, 20062−20071.

[S3] C. M. Aitchison, M. Sachs, M. Little, L. Wilbraham, N. J. Brownbill, C. M. Kane, F. Blanc, M. A. Zwijnenburg, J. R. Durrant, R. S. Sprick and A. I. Copper, *Chem. Sci.*, 2020, **11**, 8744−8756.

[S4] D. J. Woods, S. J. Hillman, D. Pearce, L. Wilbraham, L.Q. Flagg, W. Duffy, I. McCulloch, J. R. Durrant, A. A. Guilbert, M. A. Zwijnenburg, R. S. Sprick and A. I. Copper, *Energy Environ. Sci.*, 2020, **13**, 1843−1855.

[S5] R. S. Sprick, Z. Chen, A. J. Cowan, Y. Bai, C. M. Aitchison, Y. X. Fang, M. A. Zwijnenburg, A. I. Copper and X. C. Wang, *Angew. Chem. Int. Ed.*, 2020, **59**, 18695−18700.

[S6] R. S. Sprick, K. J. Cheetham, Y. Bai, J. A. Fernandes, M. Barnes, J. W. Bradley and A. I. Cooper, *J. Mater. Chem. A*, 2020, **8**, 7125−7129.